Modulation of the Interparticle Spacing and Optical Behavior of Nanoparticle Ensembles Using a Single Protein Spacer

Ayush Verma, Sudhanshu Srivastava, and Vincent M. Rotello*

Department of Chemistry, University of Massachusetts, Amherst, Massachusetts 01003

Received July 8, 2005. Revised Manuscript Received October 4, 2005

Proteins provide versatile mediators for assembling nanoparticles into organized composites. Here, we demonstrate that a single protein spacer (lysozyme) can be used to direct the self-assembly of gold mixed monolayer protected clusters into controlled ensembles with varied functional response. This efficient self-assembly process provides nanocomposites featuring tunable interparticle spacings, as determined through small angle X-ray scattering, varied sample morphology, as observed by transmission electron microscopy, and modular collective optical behavior, as examined through UV−visible spectroscopic measurements.

Introduction

Nanoparticles display an array of unique magnetic, optical,[1] and electronic properties.[2] Engineered approaches can be utilized to control and apply these properties through multiscale ordering of nanoparticle ensembles[3] for the creation of nanoscale devices. Recent studies have explored the use of organic molecular and macromolecular scaffolds such as polymers,[4] dendrimers,[5] and mutidentate thioethers[6] to assemble nanoparticles into ordered solid composites. An alternative approach is the directed assembly of nanoparticles using biomacromolecules, such as proteins, exploiting the diversity of available protein systems.

Recent reports detail the use of proteins to build supramolecular hybrid structures of nanoparticles for applications such as sensing, fabrication of nanoparticle networks, analyte detection, biotemplating, and therapeutic applications.[7] Examples include the use of strepavidin and biotin to form macroscopic gold nanoparticle assemblies[8] and the use of bacterial S-layers to grow nanoparticles in a regular array.[9] However, the use of protein mediators to tune the physical characteristics such as the interparticle spacing and the assembly morphology along with the modulation of collective functional response in organized nanoparticle ensembles remains largely unexplored. In previous studies, we have demonstrated the use of protein surface recognition to control interparticle spacings based on differential stabilities of proteins.[10] This alternate use of proteins for tuning of interparticle distance, assembly morphology, and collective functional behavior of nanoparticle ensembles could provide an advantageous assembly strategy, which could pave the way for creation of new materials. Proteins can be found in a wide variety of shapes and sizes (commensurate with nanoparticles), featuring different inherent properties such as structural stability and adsorption characteristics coupled with unique functional properties such as catalysis and redox behavior. These attributes of proteins can be potentially combined with tunable nanoparticle features (size, surface functionality, and core properties)[11] to mediate generation of novel hybrid materials. Additionally, proteins allow for an efficient and cost-effective tool for generation of nanopar-

* To whom correspondence should be addressed. E-mail: rotello@chem.umass.edu.

(1) (a) Kreilbig, U.; Vollmer, M. *Optical Properties of Metal Clusters*; Springer-Verlag: Berlin, 1996. (b) Wei, A. *Nanoparticles Building Blocks for Nanotechnology*; Rotello, V. M., Ed.; Kluwer Academic/Plenum Publishers: New York, 2004; pp 173−200.

(2) (a) Ingram, R. S.; Hostetler, M. J.; Murray, R. W.; Schaaff, T. G.; Khoury, J. T.; Whetten, R. L.; Bigioni, T. P.; Guthrie, D. K.; First, P. N. *J. Am. Chem. Soc.* **1997**, *119*, 9279−9280. (b) Terrill, R. H.; Postlethwaite, T. A.; Chen, C.-h.; Poon, C.-D.; Terzis, A.; Chen, A.; Hutchison, J. E.; Clark, M. R.; Wignall, G.; Londono, J. D.; Superfine, R.; Falvo, M.; Johnson, C. S., Jr.; Samulski, E. T.; Murray, R. W. *J. Am. Chem. Soc.* **1995**, *117*, 12537−12548. (c) Chen, S.; Ingram, R. S.; Hostetler, M. J.; Pietron, J. J.; Murray, R. W.; Schaaff, T. G.;. Khoury, J. T.; Alvarez, M. M.; Whetten, R. L. *Science* **1998**, *280*, 2098−2101. (d) Daniel, M.-C.; Astruc, D. *Chem. Rev.* **2004**, *104*, 293−346. (e) Schmid, G.; Simon, U. *Chem. Commun.* **2005**, (6), 697−710.

(3) Wang, D. Y.; Mohwald, H. *J. Mater. Chem.* **2004**, *14*, 459−468.

(4) (a) Boal, A. K.; Ilhan, F.; DeRouchey, J. E.; Thurn-Albrecht, T.; Russell, T. P.; Rotello, V. M. *Nature* **2000**, *404*, 746−748. (b) Boal, A. K.; Rotello, V. M. *J. Am. Chem. Soc.* **2002**, *124*, 5019−5024. (c) Boal, A. K.; Frankamp, B. L.; Uzun, O.; Tuominen, M. T.; Rotello, V. M. *Chem. Mater.* **2004**, *16* (17), 3252−3256.

(5) Frankamp, B. L.; Boal, A. K.; Rotello, V. M. *J. Am. Chem. Soc.* **2002**, *124* (51), 15146−15147.

(6) (a) Maye, M. M.; Chun, S. C.; Han, L.; Rabinovich, D.; Zhong, C.-J. *J. Am. Chem. Soc.* **2002**, *124* (18); 4958−4959. (b) Maye, M. M.; Luo, J.; Lim, I.-I. S.; Han, L.; Kariuki, N. N.; Rabinovich, D.; Liu, T. B.; Zhong, C. J. *J. Am. Chem. Soc.* **2003**, *125* (33), 9906−9907. (c) Maye, M. M.; Lim, I.-I. S.; Luo, J.; Rab, Z.; Rabinovich, D.; Liu, T.; Zhong, C. J. *J. Am. Chem. Soc.* **2005**, *127* (5), 1519−1529.

(7) (a) Niemeyer, C. M. *Angew. Chem., Int. Ed.* **2001**, *40* (22), 4128−4158. (b) Niemeyer, C. M. *Angew. Chem., Int. Ed.* **2003**, *42* (47), 5796−5800. (c) Mann, S.; Shenton, W.; Li, M.; Connolly, S.; Fitzmaurice, D. *Adv. Mater.* **2000**, *12* (2), 147−150. (d) Katz, E.; Willner, I. *Angew. Chem., Int. Ed.* **2004**, *43* (45), 6042−6108. For the use of DNA to assemble nanoparticles see: (e) Park, S. J.; Lazarides, A. A.; Storhoff, J. J.; Pesce, L.; Mirkin, C. A. *J. Phys. Chem. B* **2004**, *108* (33), 12375−12380. (f) Park, S. J.; Lazarides, A. A.; Mirkin, C. A.; Letsinger, R. L. *Angew. Chem., Int. Ed.* **2001**, *40* (15), 2909−2912. (g) Loweth, C. J.; Caldwell, W. B.; Peng, X. G.; Alivisatos, A. P.; Schultz, P. G. *Angew. Chem., Int. Ed.* **1999**, *38* (12), 1808−1812.

(8) Connolly, S.; Fitzmaurice, D. *Adv. Mater.* **1999**, *11* (14), 1202−1205.

(9) Shenton, W.; Pum, D.; Sleytr, U. B.; Mann, S. *Nature* **1997**, *389* (6651), 585−587.

(10) Srivastava, S.; Verma, A.; Frankamp, B. L.; Rotello, V. M. *Adv. Mater.* **2005**, *17* (5), 617−621.

10.1021/cm051483e CCC: $30.25
Published on Web 11/12/2005

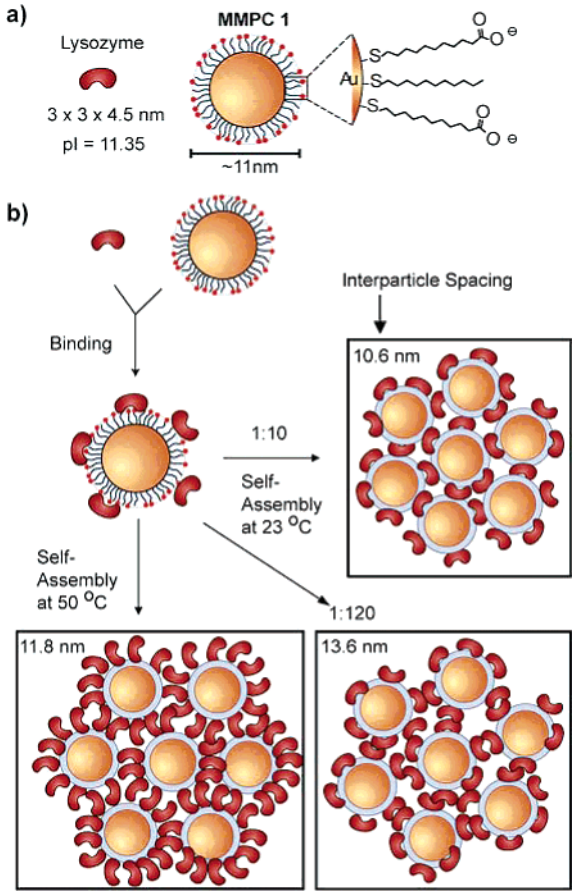

Figure 1. (a) Relative sizes of lysozyme and **MMPC 1**. (b) Schematic representation of the self-assembly process at the different temperatures featuring various protein−MMPC assembly modes. The interparticle spacing obtained from each self-assembly mode is provided in the respective inset.

ticles ensembles with a greater choice range of interparticle spacings (a key factor in determining optical, electronic, and magnetic response in nanoparticle composites) as compared to organic scaffold-mediated nanoparticle assemblies.[4−6]

Here, we report a facile self-assembly strategy utilizing a single protein spacer to dictate gold mixed monolayer protected clusters (MMPCs) into well-ordered composites with a control over assembly morphology, larger interparticle spacings, and variable collective optical behavior of the ensembles (Figure 1). For our studies, we used lysozyme, a well-characterized and globular protein, which is resistant to denaturation.[12] Adsorption studies of lysozyme on negatively charged silica surfaces have been extensively examined in the literature;[13] the study by Penfold et al. has displayed concentration dependence multilayer formation of the protein on silica surfaces,[13a] while Czeslik et al. have displayed a temperature-dependent modulation of lysozyme orientation on silica.[13c] These results provided the opportunity to harness the unique protein adsorption behavior for efficient and modular self-assembly of gold nanoparticles using a single spacer. In our studies, we demonstrate that lysozyme can be used as a mediator to dictate the physical characteristics of the assembly as well as modulate the functional behavior in the nanoparticle ensembles. Significantly, when the protein−MMPC stoichiometry and the temperature of the assembly are controlled, the self-assembly process can be directed to tune the interparticle spacings as determined through small angle X-ray scattering (SAXS), the composite morphology as examined by transmission electron microscopy (TEM), and the collective optical response as displayed via UV−visible spectroscopic measurements. Additionally, this methodology allows the segregation of the particle spacing from the functional behavior of the assembly, displaying a unique level of control achieved via the protein-mediated self-assembly process.

Experimental Section

General. Chicken egg white lysozyme was purchased from Sigma-Aldrich Chemical Co. The extinction coefficient of lysozyme at 280 nm was taken to be 38940 M^{-1} cm^{-1} for concentration determination.[14] Lysozyme stock solution was prepared at 456 μM, while **MMPC 1** stock solution was kept at 2.1 μM. **MMPC 1**, featuring a core diameter of 6.8 nm, was synthesized using our previously published procedure.[15] The nanoparticle/protein composites obtained at 1:120 molar ratio were photographed using a white light source. All the experiments were carried out in Milli-Q water. Nanoparticles from the same batch were used for all experiments.

Small-Angle X-ray Scattering (SAXS). A 0.6 cm^2 piece of Kapton film was placed at the bottom of a 2 mL vial. Then 88.24 μL of **MMPC 1** (2.1 μM) was added to lysozyme solutions (preincubated in water at 23 and 50 °C) in the vials to obtain final **MMPC 1**/protein ratios of 1:10 at 23 °C and 1:30, 1:60, 1:90, and 1:120 at both 23 and 50 °C. The final volume of all solutions was kept at 1 mL. All the samples were incubated for 12 h at the respective temperatures, during which complete precipitation of the MMPC−protein complex was observed. Thereafter, the supernatant was removed, providing thin films of **MMPC 1**−protein nanocomposites. The **MMPC 1** sample was prepared by placing a few drops of the nanoparticle stock solution on the Kapton film and allowing slow evaporation at the desired temperature.

Protein Uptake Studies. To determine the relative amount of lysozyme taken up upon assembly, samples were prepared in a manner identical to the SAXS samples in 1.5 mL eppendorf tubes. Upon assembly, the samples were centrifuged for ~1 min, after which the supernatant containing the unassembled protein was collected and the concentration determined through absorbance measurements at 280 nm using the extinction coefficient of lysozyme.[14]

Transmission Electron Microscopy (TEM). TEM samples were prepared under identical conditions as the SAXS samples (except the total sample volume was 200 μL) by placing a Cu carbon TEM

(11) Hostetler, M. J.; Wingate, J. E.; Zhong, C.-J.; Harris, J. E.; Vachet, R. W.; Clark, M. R.; Londono, J. D.; Green, S. J.; Stokes, J. J.; Wignall, G. D.; Glish, G. L.; Porter, M. D.; Evans, N. D.; Murray, R. W. *Langmuir* **1998**, *14* (1), 17−30.
(12) (a) Haynes, C. A.; Norde, W. *Colloid Surf., B* **1994**, *2*, 517−566. (b) Privalov, P. L.; Khechinashvili, N. N. *J. Mol. Biol.* **1976**, *86*, 665−684. (c) Norde, W.; Anusiem, A. C. I. *Colloids Surf.* **1992**, *66*, 73−80.
(13) (a) Su, T. J.; Lu, J. R.; Thomas, R. K.; Cui, Z. F.; Penfold, J. *Langmuir* **1998**, *14* (2), 438−445. (b) Su, T. J.; Lu, J. R.; Thomas, R. K.; Cui, Z. F.; Penfold, J. *J. Colloid Interface Sci.* **1998**, *203* (2), 419−429. (c) Jackler, G.; Steitz, R.; Czeslik, C. *Langmuir* **2002**, *18* (17), 6565−6570. (d) Czeslik, C.; Winter, R. *Phys. Chem. Chem. Phys.* **2001**, *3* (2), 235−239. (e) Czeslik, C.; Royer, C.; Hazlett, T.; Mantulin, W. *Biophys. J.* **2003**, *84* (4), 2533−2541. (f) Robeson, J. L.; Tilton, R. D. *Langmuir* **1996**, *12* (25), 6104−6113.
(14) Gill, S. C.; Vonhippel, P. H. *Anal. Biochem.* **1989**, *182* (2), 319−326.
(15) Carroll, J. B.; Frankamp, B. L.; Srivastava, S.; Rotello, V. M. *J. Mater. Chem.* **2004**, *14* (4), 690−694.

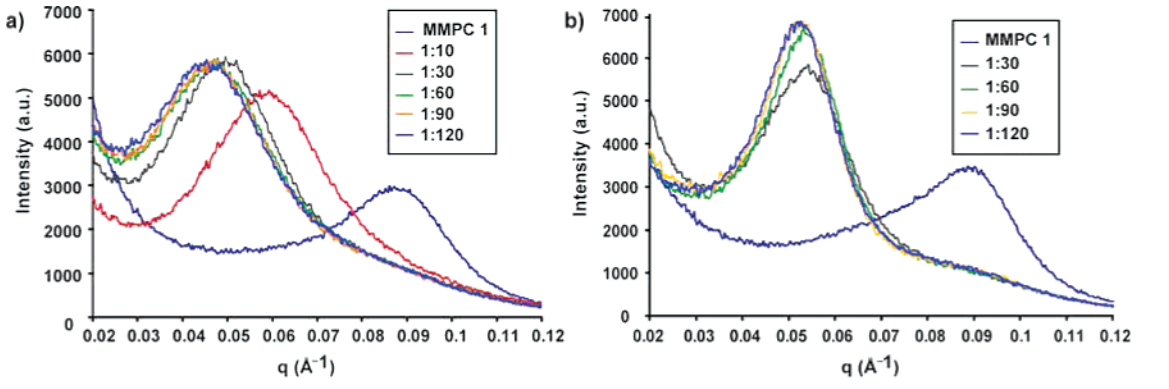

c)

MMPC 1: Protein Ratio	23 °C		50 °C	
	q (Å^{-1})	*D* (nm)	*q* (Å^{-1})	*D* (nm)
1:0	.086	7.3	.086	7.3
1:10	.059	10.6	—	—
1:30	.049	12.6	.053	11.8
1:60	.046	13.4	.053	11.8
1:90	.046	13.5	.052	12.0
1:120	.046	13.6	.051	12.1

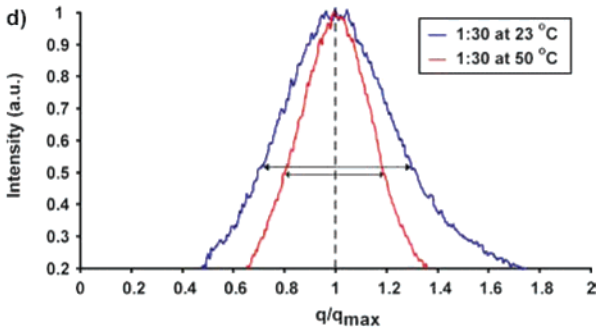

Figure 2. SAXS plot for the protein−nanoparticle composites at (a) 23 °C and (b) 50 °C. (c) The interparticle spacing increases from 7.3 to 13.6 nm at the lower temperature; however, almost a constant spacing is observed at the higher temperature at all the **MMPC 1**:protein ratios studied. (d) SAXS plot for 1:30 nanoparticle/protein ratio after background subtraction and normalization displays lower spacing distribution in the higher temperature sample.

grid (300 mesh) inside a 2 mL vial and allowing complete precipitation, after which the supernatant was removed. The samples were then analyzed by a JEOL 100CX electron microscope with an accelerating voltage of 100 k eV.

Optical Studies. A 1 cm^2 piece of Mylar film was placed at the bottom of a 7 mL vial. Identical to the samples prepared for SAXS (except the total volume was 300 μL), the assembly process was carried out at the two temperatures and the films were obtained after complete precipitation and removal of the supernatant. For a **MMPC 1**/protein ratio of 1:120, samples for the optical studies were prepared at additional temperatures of 30, 40, and 45 °C. Before the absorbance spectra of the solid nanocomposites were recorded, a fresh Mylar film was used as a blank. For the absorbance measurement of the nanoparticles in solution, a final concentration of 1 μM of **MMPC 1** was placed in a quartz cuvette with 1 cm path length. All absorbance measurements were performed using a UV-spectrophotometer (HP 8452A).

Results and Discussion

For our studies, we used lysozyme, an ellipsoidal protein with dimensions 3 × 3 × 4.5 nm.[16] The protein has a very high isoelectric point (pI = 11.35),[17] making the surface overall positively charged and hence suitable for assembly with negatively charged nanoparticles through complementary electrostatic surface interactions.[18] Upon incubation, the protein bound to the carboxylate-functionalized MMPCs acts as a multidentate linker, thereby cross-linking the MMPCs in solution and resulting in precipitation of the complex via a self-assembly process. The protein-mediated assembly was conducted at various MMPC−protein stoichiometries ranging from 1:10 to 1:120 molar ratios and at two different temperatures, 23 and 50 °C,[19] for modulation of the physical characteristics and the collective functional behavior of the ensembles.

Temperature-Dependent Control of Interparticle Spacing. SAXS was employed to provide evidence of ordering and for quantification of the interparticle spacings in the protein−nanoparticle solid composites obtained at two different temperatures, 23 and 50 °C. MMPCs were added to solutions containing varying amounts of excess protein (required for the precipitation) to achieve final MMPC−protein molar ratios ranging from 1:10 to 1:120 at 23 °C and from 1:30 to 1:120 at 50 °C. As a control, a solid sample of MMPC was prepared to provide particles spaced by their monolayer only. The SAXS plot (Figure 2a and b) demonstrates that assemblies obtained at both temperatures feature well-defined interparticle spacings. However, distinctive differences are observed in particle spacings in the assemblies obtained at the two different temperatures. In protein−nanoparticle ensembles prepared at the lower (room) temperature, an increase in the particle spacing is observed with an increase in the nanoparticle−protein stoichiometry. At the lowest protein concentration, an increase in spacing of 3.3 nm is observed (Figure 2c). However, upon progressive addition of excess protein (up to 1:120 nanoparticle/protein ratio), the interparticle distance increases up to 6.3 nm. This observation is consistent with the studies of lysozyme

(16) Creighton, T. E. *Proteins*; Freeman, W. H.: New York, 1993.
(17) Wetter, L. R.; Deutsch, H. F. *J. Biol. Chem.* **1951**, *192* (1), 237−242.
(18) Complementary surface interactions between proteins and MMPCs have been used in our earlier studies for control of protein activity and structure. See (a) Fischer, N. O.; McIntosh, C. M.; Simard, J. M.; Rotello, V. M. *Proc. Natl. Acad. Sci. U.S.A.* **2002**, *99*, 5018−5023. (b) Verma, A.; Simard, J. M.; Worrall, J. W. E.; Rotello, V. M. *J. Am. Chem. Soc.* **2004**, *126* (43), 13987−13991.
(19) The rate of precipitation was observed to be higher for the assembly process at 50 °C as compared to that at the lower temperature.

adsorption on silica surfaces, which display that, at room temperature and at lower protein concentrations, side-on adsorption of lysozyme is observed on silica surfaces, with the long axis parallel to the negatively charged surface. However, enhanced concentrations of lysozyme result in a bilayer side-on adsorption with minimum loss of protein structure.[13a] The SAXS results, therefore, display that a single spacer can be utilized to tune the increase in interparticle distance from 7.3 nm (no protein) up to 13.6 nm through this self-assembly method. Significantly, it is difficult to achieve such a large increase in interparticle spacings via organic scaffold-mediated self-assembly methods.

To demonstrate a complementary control over particle spacing and the resultant collective behavior of the assembled nanocomposites, the protein-mediated self-assembly was performed at 50 °C. Precedents have displayed that, at higher temperatures, a monolayer adsorption of lysozyme occurs in an end-on orientation on silica surfaces along with a denser protein packing on the surface.[13c] As a result, efficient and complete precipitation was not observed for 1:10 **MMPC 1**:protein ratio at the higher temperature. Additionally, non-cross-linked lysozyme molecules adsorbed onto negatively charged surfaces at higher temperatures display a collapsed or highly flexible tertiary structure,[20] which is amenable to protein intermolecular associations and can serve as sites for deposition of other protein molecules.[21] However, electrostatic cross-linking of the protein with the nanoparticles is expected to provide little conformational freedom, thereby allowing particles spaced by the protein edge length.[22] In our studies, similar to the assembly procedure at the lower (room) temperature, MMPCs were added to the varying amounts of protein to obtain final particle−protein ratios ranging from 1:30 to 1:120 at 50 °C. All the samples studied at the higher temperature displayed an increase in spacing of about 4.5 nm by SAXS (Figure 2c), consistent with lysozyme adsorbing in an end-on orientation, thereby spacing particles by the long edge of the protein. Interestingly, background subtraction and normalization of the SAXS plots observed at the two different temperatures (1:30 in Figure 2d) displayed that a lower spacing distribution concomitant with better ordering of the nanoparticles was observed with the samples assembled at the higher temperature.

Protein Uptake. To correlate the amount of protein taken up during the assembly with the interparticle spacings and the optical behavior of the ensembles, centrifugation assays were performed for all the samples at the different temperatures to determine the ratio of **MMPC 1** and protein present in the nanocomposites.[23] In the samples prepared at both temperatures, increased protein uptake was observed with the increasing initial particle/protein stoichiometry. In samples prepared at 23 °C, the rate of protein uptake is higher at the lower stoichiometries, while becoming constant at greater nanoparticle/protein ratios, reflecting the trend observed in the SAXS data. At the higher temperature, although the particles are spaced by almost the same distance at all three ratios, the relative amount of protein uptake was found to increase consistently with increase in the initial protein−particle ratio. This trend is reflected with the shift in the λ_{max} of the SPR, as demonstrated later through the UV−visible studies, correlating the trend in the collective optical response of the composites with the loss of protein concentration upon assembly.

Table 1. Ratios of Nanoparticle and Protein Present in the Composites after the Self-assembly Process at Different Initial Stoichiometries and Temperatures, as Determined by Residual Protein in Solution after Precipitation

MMPC 1: Protein Ratio

	in assembled samples	
before assembly	23 °C	50 °C
1:10	1:9	
1:30	1:24	1:29
1:60	1:38	1:58
1:120	1:38	1:70

Morphological Differences in Samples. Samples prepared at different temperatures via the protein-mediated self-assembly approach display differences in macroscopic as well as mesoscopic morphology. The reflectance of the films obtained at the two different temperatures for **MMPC 1**:protein ratio of 1:120 has been shown in the insets of Figure 3b and d. The composites prepared at lower temperature display brownish aggregates; however, at the higher temperature, the nancomposites display a smooth purplish film. A closer examination of the protein−nanoparticle ensembles through TEM (Figure 3) displays that the samples prepared at higher temperature feature a compact structure as opposed to a relatively extended morphology for the lower temperature samples. Additionally, due to enhanced intermolecular protein interactions at the higher temperature,[21] an increase in protein uptake by the assembly is expected (as confirmed through protein uptake studies), resulting in a gray border around the assembly, as seen in Figure 3d.[24] Significantly, the higher protein amount around the composites increases the local refractive index of the environment,[25] resulting in two contrasting assembly modes for protein−nanoparticle ensembles, which leads to modulation of the collective optical response in these ensembles, as displayed in the insets and as examined subsequently via optical studies.

(20) Vanstokkum, I. H. M.; Linsdell, H.; Hadden, J. M.; Haris, P. I.; Chapman, D.; Bloemendal, M. *Biochemistry* **1995**, *34* (33), 10508−10518.

(21) (a) Ball, A.; Jones, R. A. L. *Langmuir* **1995**, *11* (9), 3542−3548. (b) Green, R. J.; Hopkinson, I.; Jones, R. A. L. *Langmuir* **1999**, *15* (15), 5102−5110.

(22) In a separate experiment, the protein−nanoparticle assemblies obtained at 23 °C were annealed to a temperature of ∼80 °C, over a 18 h period. Thereafter, SAXS performed on the annealed samples did not show any change in the interparticle spacings, displaying the robust nature of assembly and the resistance of cross-linked protein against denaturation by heat.

(23) Due to the nature of the assembly obtained, it is difficult to determine the exact thickness of bound protein and correlate it quantitatively to the surface plasmon peaks.

(24) **MMPC 1**, alone, was kept in solution at 50 °C for overnight. No change in the absorbance maxima or aggregation in solution was observed, displaying that the nanoparticles were stable under the assembly conditions at the higher temperature.

(25) For intermolecular protein interactions, the increase in the local refractive index is proportional to the amount of molecules bound. See: Quinn, J. G.; O'Neill, S.; Doyle, A.; McAtamney, C.; Diamond, D.; MacCraith, B. D.; O'Kennedy, R. *Anal. Biochem.* **2000**, *281* (2), 135−143.

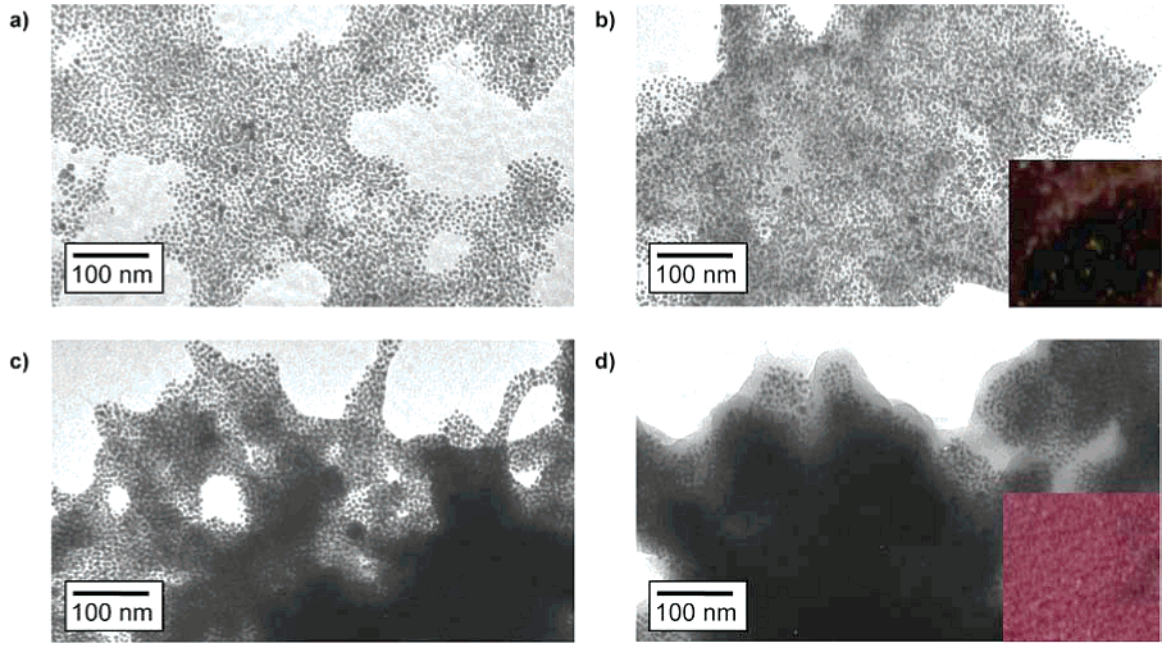

Figure 3. TEM images of the protein nanocomposites. (a) 1:30 and (b) 1:120 at 23 °C, (c) 1:30, and (b) 1:120 at 50 °C. Insets display the reflected colors and the differences in macroscopic morphology for the respective films.

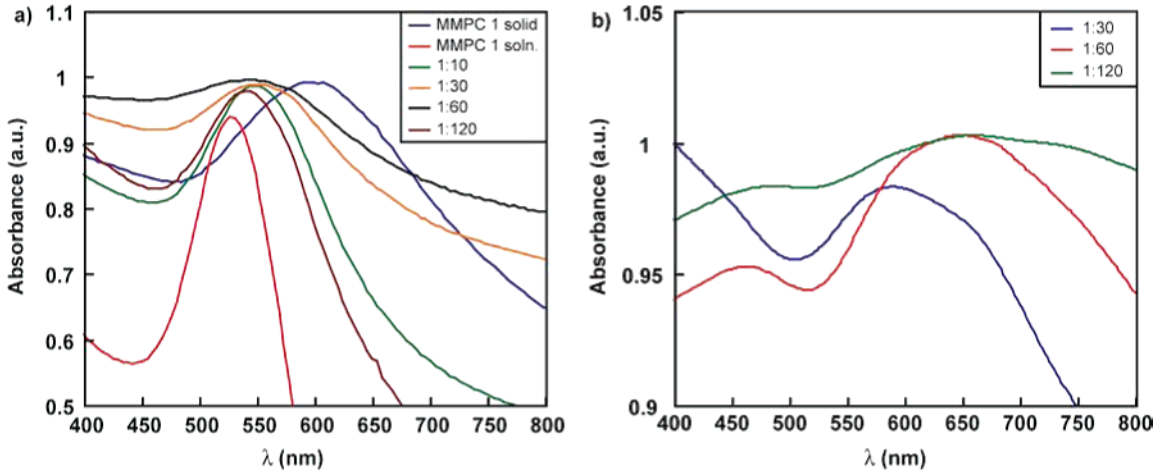

c)

λ_{max} (nm)	23 °C	50 °C
1:10	548	—
1:30	546	598
1:60	542	653
1:120	542	675
MMPC 1 Solid	596	
MMPC 1 Soln.	528	

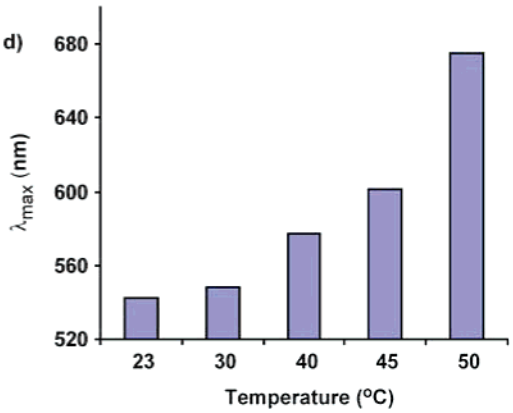

Figure 4. The optical response for the protein−nanocomposites solid films displayed at (a) 23 °C and (b) 50 °C. The ratios indicate **MMPC 1**:protein stoichiometries and **MMPC 1** soln. refers to only nanoparticles in water. (c) Minimum variation in λ_{max} is obtained with the assemblies at the lower temperature; however, >75 nm shift in the wavelength is seen at the higher temperature. The λ_{max} for each sample was obtained through curve fitting. (d) 127 nm shift in λ_{max} is obtained through a particle/protein ratio of 1:120, assembled at the different temperatures.

Optical Response. UV−visible spectroscopy was used to analyze the surface plasmon resonance (SPR)[1] of the solid nanocomposites upon assembly at various temperatures, demonstrating the modulation of dipolar optical interactions,[26] as shown in Figure 4. The optical responses of **MMPC 1** in solution (assumed to be free of dipolar coupling) and nanoparticles displaying maximum coupling (spaced only by the monolayer) were monitored. It was observed that the

λ_{max} of free nanoparticles in solution was 528 nm, while the nanoparticles spaced only by the monolayer displayed a SPR of 596 nm, due to an increased dipolar coupling. Interestingly, minimal variation of the collective optical response (from 542 nm at 1:120 particle−protein ratio to 548 nm at 1:10 ratio) in the samples prepared at the lower temperature was observed, even upon a large increase in the interparticle spacing (by 6.3 nm). Such a large increase in spacing is expected to result in a substantial blue shift of the λ_{max}, thereby approaching the wavelength of free nanoparticles in solution, as observed in our previous studies using different generation dendrimers to space MMPCs.[27] However, with the increase in spacings, more protein contained between nanoparticles results in an increased refractive index of the surrounding environment,[25] which is well-known to induce a red-shift of the SPR of metal nanoparticles.[28] The net result is a nominal blue shift, even at the higher spacings. Interestingly, this demonstrates that nanoparticles can be spaced at larger distances with minimum effect on the optical response of the ensembles. Conversely, the larger interparticle distances achieved via this method can be used for modulation for collective properties between nanoparticles featuring bigger core sizes and also properties that are not dependent on the refractive index of the spacer, such as magnetic coupling between paramagnetic nanoparticles.

A complementary level of control over the collective optical response was achieved using the assembly formed at higher temperature. While the effect of increased refractive index induces a moderate red-shift in the SPR of the *individual* nanoparticles, the *collective* SPR of the coupled nanoparticles is highly sensitive to the refractive index of the surrounding environment. This has been recently studied by Tsukruk et. al., where they have displayed that a few nanometers thick film of polymers coated onto a film of optically coupled gold nanoparticles can red-shift the collective SPR of the assembly by 90 nm.[29] This behavior, combined with the unique protein−MMPC self-assembly mode at the higher temperature, was exploited to direct the collective response in the hybrid nanocomposites, via the self-assembly process. Samples prepared at 50 °C featured particles spaced by a particular distance, which ensured a constant dipolar coupling for the higher temperature ensembles. However, an increase in the amount of protein around the assembly with increasing nanoparticle:protein ratio is expected to enhance the local refractive index, resulting in a significant red-shift of the collective plasmon peak.[28] As expected, the collective plasmon peak was found to be dependent on the particle/protein ratio (Figure 4). The absorbance spectra display that the λ_{max} of the protein−nanoparticle composites is red-shifted, even beyond the particles separated only by their monolayer. The collective response of the assembly was found to be dependent on the excess protein used, with the highest ratio shifting the SPR to 675 nm.[30] Additionally, MMPC−protein composites (1:120) assembled at various temperatures displayed that the collective plasmon peak can be tuned over a 127 nm range (from 548 to 675 nm), through this efficient self-assembly methodology (Figure 4d). This can be explained by studies in the literature, which have shown that the adsorption of non-cross-linked lysozyme molecules on silica surfaces increases progressively with an increase in temperature from 25 to 55 °C at a particular concentration of lysozyme.[13c] This factor is expected to contribute to the shift in the SPR of the assembled nanoparticles. Additionally, SAXS measurements at an intermediate temperature (40 °C) revealed that the increase in the interparticle spacing was 5.6 nm, which suggests that there might be a gradual decrease in the particle spacing at 1:120 particle/protein ratio in going from 23 °C (6.3 nm) to 50 °C (4.5 nm) during the assembly process. This will contribute as well to the increase in dipolar coupling and the subsequent red-shift observed.

Conclusion

In summary, we have demonstrated that a single protein spacer can be utilized for modular and efficient self-assembly of nanoparticles into controlled composites. The self-assembly process can be directed to feature large interparticle spacings, varied morphology, and tunable collective optical response in the ensembles. Significantly, with use of this methodology, the interparticle spacings can be segregated from the collective optical response in the biomaterial, thereby demonstrating a unique level of control in the self-assembly process. This work displays one of the potential benefits in using proteins for directing the self-assembly of nanoparticles and can be extended toward assembly of gold nanoparticles with bigger core sizes or the self-assembly of magnetic nanoparticles for tuning of collective optical or magnetic response in the biomaterials. Importantly, this work displays the integration of an inherent protein property with functional response in nanoparticle composites.

Acknowledgment. This research was supported by the National Institutes of Health (NIH, GM 59249) and National Science Foundation (NSF, CHE-0518487 and MRSEC facilities). We thank Alexander Wei (Purdue) for helpful conversations.

CM051483E

(26) (a) Saponjic, Z. V.; Csencsits, R.; Rajh, T.; Dimitrijevic, N. M. *Chem. Mater.* **2003**, *15* (23), 4521−4526. (b) McConnell, W. P.; Novak, J. P.; Brousseau, L. C., III.; Fuierer, R. R.; Tenent, R. C.; Feldheim, D. L. *J. Phys. Chem. B.* **2000**, *104* (38), 8925−8930.

(27) Srivastava, S.; Frankamp, B. L.; Rotello, V. M. *Chem. Mater.* **2005**, *17* (3), 487−490.

(28) (a) Mulvaney, P.; *Langmuir* **1996**, *12* (3), 788−800. (b) Yonzon, C. R.; Jeoung, E.; Zou, S.; Schatz, G. C.; Mrksich, M.; Van Duyne, R. P. *J. Am. Chem. Soc.* **2004**, *126* (39), 12669−12676.

(29) Jiang, C.; Markutsya, S.; Tsukruk, V. V. *Langmuir* **2004**, *20* (3), 882−890.

(30) For the samples assembled at higher temperatures, additional absorbance peaks at ∼460 nm are observed. The origin of these peaks is unknown at present and could be due to either local dielectric effects or short-range anisotropy in the assembly process.